PerTPV – Perovskite thin film photovoltaics

Grant agreement 763977

Deliverable 5.1

Single junction demonstrator mini-module (100 cm2) with an efficiency of 20% based on the first stage materials set, with less than 350 µm “dead area” within the P1-P2 and P3 cell interconnection region

WP5

Lead beneficiary: CSEM

Authors: Adriana Paracchino, Soo-Jin Moon, Sylvain Nicolay

Delivery date: 01/04/2020

Confidentiality level: Public

Revision History

Author Name, Partner short name	Description	Date
Adriana Paracchino, CSEM	Draft deliverable	23/03/2020
Henry Snaith, UOXF	Revision 1	26/03/2020
Henry Snaith, UOXF	Final version	26/03/2020

Contents

REVISION HISTORY **2**

CONTENTS **2**

1. INTRODUCTION **3**

2. EXPERIMENTS **5**

2.1. OPTIMISATION OF LASER SCRIBING CONDITIONS 5
2.2. PEROVSKITE MODULES FABRICATION AND RESULTS 6

3. CONCLUSIONS **8**

1. Introduction

Highly efficient 100 cm^2 mini-modules surpassing 20% efficiency are realistically possible if the efficiency of 1 cm^2 devices is close to the state-of-the-art efficiency, which is 25.2%,[1] or at least around 23%. Indeed, film inhomogeneities, interconnection area losses and sheet resistance losses are to be accounted for in upscaling from 1 cm^2 cells to large area modules and will lower the module efficiency. For example, the largest perovskite module reported so far (354 cm^2) achieved an efficiency of 12.6% while the 0.04 cm^2 device fabricated in the same laboratory was at 15.4%.[2] Thus the first step towards high efficiency modules is to reach high efficiency at the 1 cm^2 scale. Record efficiency perovskite devices have minimal non-radiative recombination losses thanks to passivation of perovskite defects in the bulk, at the grain boundaries and at the interfaces between the perovskite and the charge-transporting layers. In order to minimize the loss of efficiency in the upscaling it is crucial on one side to control the perovskite crystallisation process as in small area devices, and on the other side also reducing the inactive area associated with the series interconnection of the cells and the sheet resistance losses of the contacts.

At CSEM we have recently increased the average efficiency of our 1 cm^2 devices to >17% by changing the hole-transporting layer and then further increased it to 18% by decreasing the perovskite bandgap from our standard 1.62 eV to 1.55 eV. For further gains in efficiency passivation strategies have to be employed.

At CSEM we prepare glass-based mini-modules (MM) using thin film deposition over the full substrate area (i.e. unpatterned area) and laser scribing techniques for the series interconnection of the cells. The laser scribing techniques are commonly used for commercial thin film solar cells and are compatible with mass production. However, the perovskite layer is at the moment deposited by spin-coating with antisolvent technique, which limits the size of the substrate that can be coated. An area of 10x10 cm^2 can still be spin coated with antisolvent but perovskite film quality on 10x10 cm^2 is inferior, as compared to a 5x5 cm^2 substrate. A 5x5 cm^2 mini-module, consisting of 5 cells connected in series, is shown in Figure 1. While CSEM is to move to perovskite blade coating in the near future, the results achieved on 5x5 cm^2 for this deliverable are expected to be readily transferable to larger area, since the major challenge of reducing the dead width to <300 µm has been addressed and FF loss is expected to be small for upscaling further.

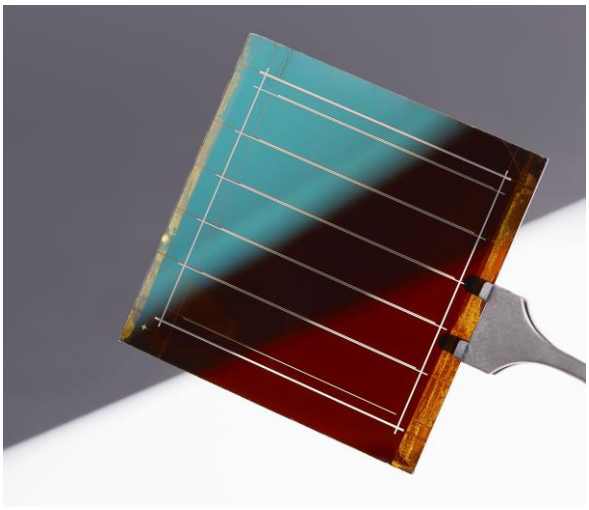

Figure 1. CSEM 5x5 cm^2 mini-module having 5 cells in series and an aperture area of 13.68 cm^2.

In order to achieve highly performing perovskite modules, power and optical losses should be minimised by reducing the interconnection area, which is inactive, and by decreasing the electrode sheet resistances, which lead to electrical losses during current extraction. To this end, using a highly selective laser process is required to increase geometric fill factor (GFF):

$$GFF = \frac{Active\ Area}{Aperture\ Area} = \frac{Wa}{Wa + Wd}$$

The Wd (dead width) corresponds to the width between the laser line P1 and the laser line P3, as represented in Figure 2. The laser process can be optimised by modifying the laser spot size, scan speed, wavelength, and power like laser current and frequency.

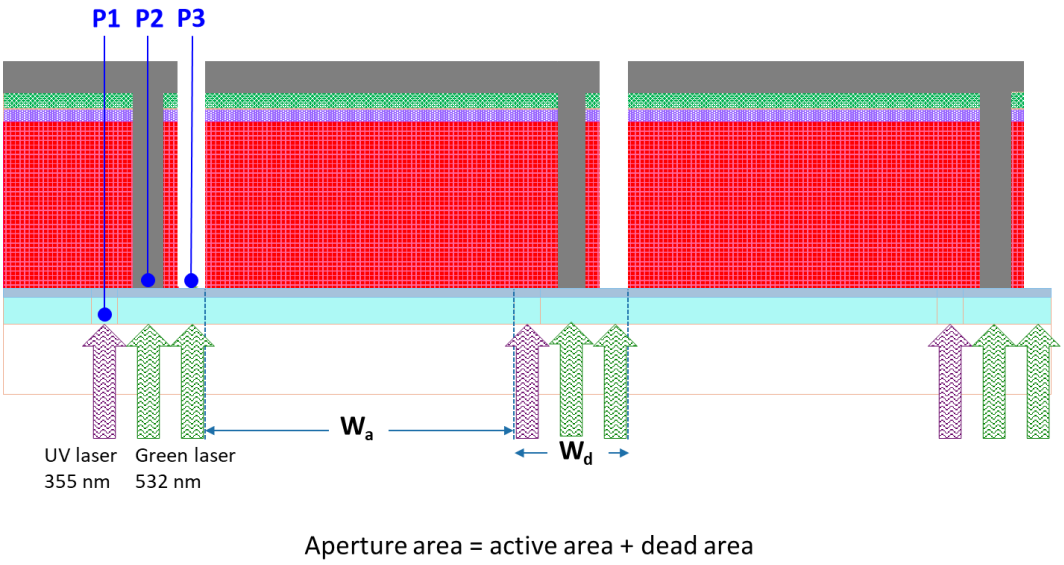

Figure 2. Schematics of the laser scribing process at CSEM. P1 is the laser scribing on the substrate TCO, prior to any deposition. P2 is the laser scribing that defines the singles cells and connects them in series once the top contact is deposited. P3 separates the cells again after top contact deposition. The P1 to P3 distance has to be minimized to achieve a high GFF, i.e. an aperture area as close as possible to the active area.

2. Experiments

2.1. Optimisation of laser scribing conditions

The P1 scribe is done by UV laser (355 nm) and test lines were made by using different pulse energies, and scribe speed at constant 30 kHz pulse frequency and fixed focal distance. TCO isolation was confirmed by multimeter. The P2 scribing was done by a green laser (532 nm, 35 kHz pulse frequency) and the parameters were chosen based on microscope investigation and visual inspection. Spot size of P2 was over 60 µm. P3 line (532 nm, 35 kHz pulse frequency) was optimised in a similar way to provide proper back contact electrical isolation, which was confirmed by the measurement of a high photovoltage under low illumination conditions.

The laser processing conditions are summarized in Table 1.

Table 1. Summary of laser process condition for perovskite module.

Interconnection line	Laser source	Pulse energy (µJ)	Scribe speed (mm/sec)
P1	UV	22-26	400-800
P2	Green	33-37	1200-1600
P3	Green	28-32	1200-1800

A confocal microscope image of the dead width is shown in Figure 3. It can be seen that the dead width is still about 400 µm. Small delamination of Ag is observable around P3, which increases the dead area, however the P3 line is free from metal flakes that would create current shunts between adjacent cells in the module.

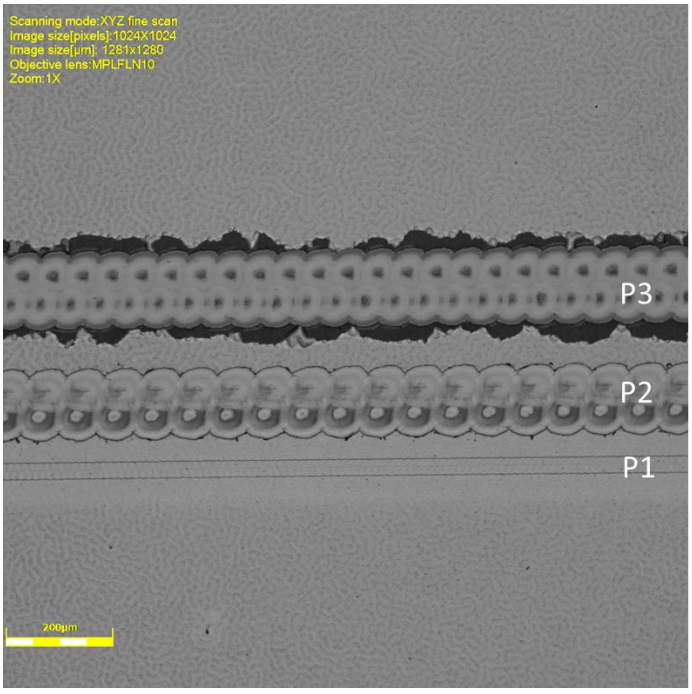

Figure 3. A confocal microscope image of P1, P2 and P3 interconnection lines.

In order to reduce the dead area to <350 µm, as required by this deliverable, we have tested a new femtosecond (fs) laser with P2 and P3 spot sizes of 35 µm, enabling narrower patterning width compared to what could be achieved with a ns laser. As shown in Figure 4, P3 shows much lower delamination compared to Figure 3 and so dead width can be reduced to <250 µm.

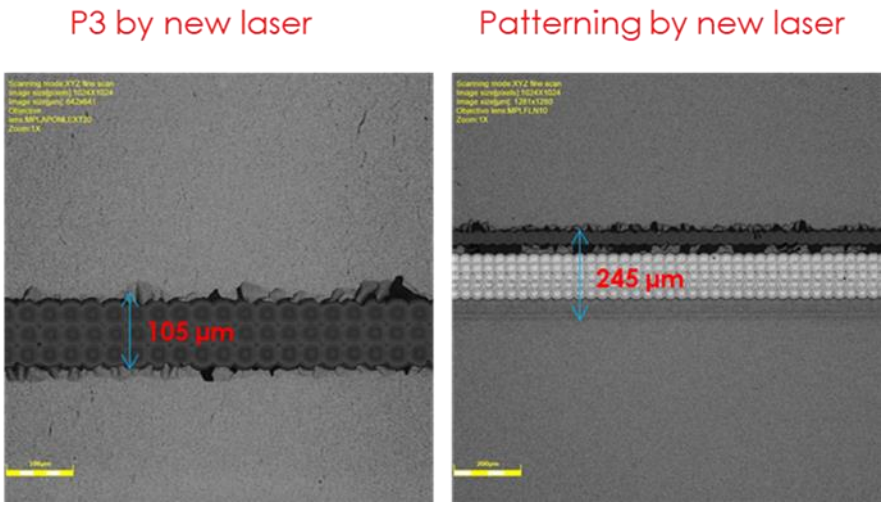

Figure 4. Confocal microscope images of P3 (left) and P1, P2, P3 interconnection lines (right).

2.2. Perovskite modules fabrication and results

Perovskite mini-modules are fabricated on commercial ITO with a sheet resistance of about 7-8 Ohm/sq. The HTM consists of a bilayer of 20 nm sputtered NiO_x and spin-coated poly-TPD (2 mg/ml). $Cs_{0.15}FA_{0.8}MA_{0.05}Pb(I_{0.95}Br_{0.05})_3$ perovskite, with a bandgap of 1.55 eV, is spin-coated with the antisolvent method inside a nitrogen-filled glovebox. 1 nm of LiF and 20 nm C60 are then thermally evaporated and a 10 nm layer of SnO_2 is deposited by thermal ALD at 100°C. The top contact consists of a stack ITO 58 nm/Ag 25 nm/ITO 47 nm and is deposited by DC sputtering. The Ag layer decreases the sheet resistance of the top contact while still providing good transparency (70% at 550 nm), as shown in Figure 5. Covering Ag with another layer of ITO has proven essential to avoid metal flaking during P3.

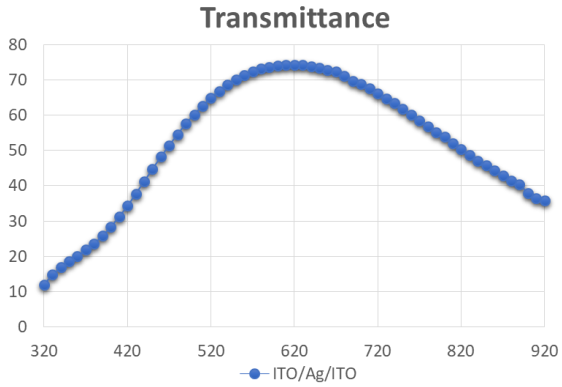

Figure 5. Transmittance of the top semi-transparent contact.

The best mini-module efficiency achieved with the laser scribing conditions reported in Table 1 is 16.1% on an aperture area of 13.7 cm^2 (Figure 6).

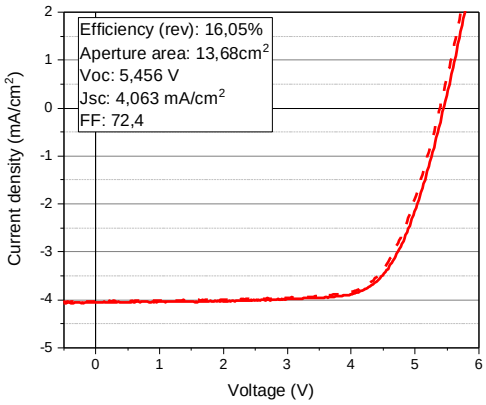

Figure 6. Current density-voltage characteristics for a semi-transparent mini-module.

With the new fs laser higher efficiencies on aperture area are expected, thanks to the higher GFF. However, due to the very limited availability of the tool at the moment we could only compare mini-modules with a less optimised perovskite solar cell stack, i.e. ITO/NiO/$Cs_{0.17}FA_{0.83}Pb(I_{0.83}Br_{0.17})_3$/LiF/C60/$SnO_2$/ITO/Ag/ITO (the perovskite used in this stack has a bandgap of 1.63 eV and the stack does not include poly-TPD). The results of the comparison are shown in Figure 7. The main gain, as expected, is in the short-circuit current, due to the smaller dead area. Therefore, by repeating the experiment with an optimised perovskite cell stack, we expect the efficiency to get close to 18% on the same aperture area.

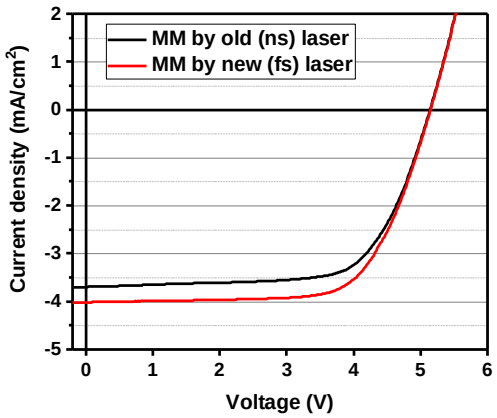

Laser type	Voc [mV]	Jsc [mA/cm2]	FF [%]	Eff @MPP [%]
MM by ns laser	5141	3.699 (subcell Jsc: 18.5)	68.26	13.1
MM by fs laser	5159	**4.019** (subcell Jsc: 20.1)	69.1	**14.74**

Figure 7. Comparison of current density-voltage characteristics and performance for mini-modules (MM) fabricated with standard laser and new laser. Aperture area: 13.68cm^2

3. Conclusions

CSEM has achieved an efficiency of >16% on a semi-transparent mini-module of 13.687 cm^2 aperture area and a dead width of 400 µm and is expected to reach close to 18% in the coming months by using a more powerful laser, which has already proved to decrease the dead width to 250 µm. The efficiency of the semi-transparent MM is very close to that achieved on 1 cm^2 devices (only 1% absolute lower), which indicates that in order to achieve >20% efficiency a breakthrough is needed on the 1 cm^2 scale to deliver comparable p-i-n structured solar cells at over 21% efficiency. This means that some of the known strategies for perovskite defects passivation have to be tested (such as alloying chlorine into the perovskite,[3] adding traces of alkylamine ligands[4] or other small molecule additives). We are also looking into improving the energy band alignment of the HTM/perovskite interface, for example by replacing the NiO with the self-assembling monolayers (SAM) HTMs developed by our PERTPV partners at Kaunas University. However, while in 1 cm^2 devices this has shown to improve V_{oc}, FF and J_{sc} (the latter thanks to higher transparency for wavelengths <420 nm when removing NiO from the stack, or reducing its thickness), the deposition of the SAMs is currently under optimisation in order to increase the yield of non-shunted devices, a necessary step before upscaling.

CSEM mini-modules are at present limited to 5x5 cm^2 area. This is entirely due to the perovskite deposition technique. Indeed, it is challenging to spin-coat on a 10x10 cm^2

substrate without perovskite discoloration, due to the large volume of solvents building up in the spin-coater, and also to reach a uniform thickness from the centre to the edges. The other deposition techniques used for the mini-modules (sputtering, thermal evaporation, ALD) can readily be used for coating on a 15x15 cm^2 substrate, making it possible to achieve aperture areas in the order of 100 cm^2. CSEM has recently acquired a blade-coater and will optimise the perovskite deposition by blade coating in the coming months.

If the width of the cells in the modules is kept the same while upscaling from 5x5 cm^2 to 10x10 cm^2, there should be no additional resistive losses, provided that the sheet resistances of the bottom ITO and top contact are low enough. In order to further lower the sheet resistance of the top contact the Ag layer in the ITO/Ag/ITO stack can be increased to benefit from the bulk conductivity of silver (in this case the top contact would be opaque instead of semi-transparent).

[1] https://www.nrel.gov/pv/cell-efficiency.html

2 Higuchi et al. Largest highly efficient 203 × 203 mm2 CH3 NH3 PbI3 perovskite solar modules, *Jpn. J. Appl. Phys*. 57 08RE11 (2018)

[3] Xu et al. Triple-halide wide–band gap perovskites with suppressed phase segregation for efficient tandems, *Science* 367, 1097–1104 (2020)

[4] Zheng et al. Managing grains and interfaces via ligand anchoring enables 22.3%-efficiency inverted perovskite solar cells. *Nat Energy* 5, 131–140 (2020).